Heterogeneous Catalysis

DOI: 10.1002/anie.201201866

# The Intimate Relationship between Bulk Electronic Conductivity and Selectivity in the Catalytic Oxidation of *n*-Butane**

*Maik Eichelbaum,* Michael Hävecker, Christian Heine, Andrey Karpov, Cornelia-Katharina Dobner, Frank Rosowski, Annette Trunschke, and Robert Schlögl*

The efficient and direct functionalization of alkanes from natural gas or future regenerative carbon-based resources is impeded by the lack of suitable catalysts and the absence of a detailed mechanistic understanding of the few efficient alkane oxidation reactions. The selective oxidation of *n*-butane to maleic anhydride (MA), an important basic chemical with an annual global production of 1.4 Mt,[1] is one of such scarce commercialized examples. The industrially used vanadium-phosphorous-oxide (VPO) catalyst enabling a maximum MA yield of 65 % mainly consists of $(V^{IV}O)_2P_2O_7$ (vanadyl pyrophosphate, VPP).[1–6] Based on experimental evidence[2,7–10] it is generally agreed that the reaction proceeds via a two-step mechanism, in which, in Step 1: "lattice" oxygen from the catalyst (or oxygen from an active surface site) is abstracted to oxidize the alkane, and in Step 2: the catalyst is subsequently reoxidized by gas-phase $O_2$. It is however still debated, whether the reaction proceeds on non-interacting single surface sites with the bulk being only an inert support, or if the bulk supplies charge carriers and oxygen.[3,4,11–15] The single-site concept[12–14] would demand spacious active sites to provide the large number of 14 electrons and seven oxygen atoms needed per converted *n*-butane molecule. In contrast, an unlimited bulk–surface charge and oxygen transfer contradicts the fundamental site-isolation principle[12–14] of selective oxidation catalysis, which presumes that the (stoichiometric) limitation and spatial isolation of active oxygen prevents the further oxidation of the desired product to $CO_x$.

Clearly, the investigation of charge-carrier dynamics in selective catalysts is of fundamental importance to disentangle the surface and bulk influence on the catalytic performance. Unfortunately, unstable (Schottky) contact resistances between catalyst particles, electrodes, and at grain boundaries hamper quantitative and sensitive electrical-conductivity investigations by DC or AC contact methods. Although such studies have provided valuable information on the electrical properties of VPO catalysts,[16–19] the direct participation of bulk charge carriers in the catalytic reaction has not been demonstrated unequivocally yet.

Herein, the disadvantages of contact methods could be circumvented by using a noncontact conductivity method based on the microwave cavity perturbation technique (MCPT). MCPT is a highly sensitive technique[20,21] allowing the non-invasive quantitative measurement of the permittivity and electrical conductivity of polycrystalline samples in a fixed-bed flow-through reactor.[22] The excitation of free charge carriers in the investigated sample by microwaves (at 9.2 GHz) in a calibrated resonant cavity enables the determination of absolute conductivity values. By measuring the change of the resonance frequency and the quality factor of the cavity with and without the sample, its complex permittivity $\varepsilon = \varepsilon_1 + i\varepsilon_2$ can be deduced (Figure 1).[20–22] The imaginary part $\varepsilon_2$ is composed of the dielectric loss, ionic, and electronic conductivity.[20] A major contribution of ionic charge carriers (e.g. O ions) is negligible because their high masses are not able to follow the high-frequency microwave excitation. In addition, no response of the real permittivity $\varepsilon_1$ of VPO to variations of the gas-phase chemical potential was observed, hence a significant influence of dielectric relaxations (through dipoles) can be excluded. Consequently, the major contribution to $\varepsilon_2$ in VPO is electronic conductivity. Moreover, pre-investigations showed that the catalyst behaves as a p-type semiconductor with an increasing conductivity in oxidizing and a decreasing conductivity in reducing mixtures (Figure S2 in the Supporting Information). These results are in agreement with contact conductivity investigations.[16–19]

According to X-ray powder diffractometry, the VPO catalyst was phase pure and consisted of vanadyl pyrophosphate (Supporting Information, Figure S1). The catalytic performance and conductivity of VPP were probed simultaneously with the in situ MCPT/GC setup at constant temperature, but in different gas mixtures and at different gas hourly space velocities (GHSV), i.e. at different reaction gas contact times. The catalyst was preheated in air to 400 °C (GHSV:

[*] Dr. M. Eichelbaum, Dr. M. Hävecker, C. Heine, Dr. A. Trunschke, Prof. Dr. R. Schlögl
Department of Inorganic Chemistry
Fritz-Haber-Institut der Max-Planck-Gesellschaft
Faradayweg 4–6, 14195 Berlin (Germany)
Fax: (49) 30-84134401
E-mail: me@fhi-berlin.mpg.de
Dr. M. Hävecker
Solar Energy Research, Helmholtz-Zentrum Berlin/BESSY II
Albert-Einstein-Strasse 15, 12489 Berlin (Germany)
Dr. A. Karpov, C.-K. Dobner, Dr. F. Rosowski
Process Research and Engineering
BASF SE, Carl-Bosch-Strasse 38, 67056 Ludwigshafen (Germany)

[**] This work has been supported by the German Federal Ministry of Education and Research (BMBF) as part of the ReAlSelOx project, grant number 033R028B. We thank Dr. Frank Girgsdies for XRD and Gisela Lorenz (both FHI) for BET measurements. The HZB staff is acknowledged for their continual support of the high-pressure electron spectroscopy activities of the FHI at BESSY II. We are very grateful to Prof. R. Stößer (Humboldt-Universität zu Berlin), Dr. M. Scheffler (Universität Stuttgart), and Dr. U. Banach (BAM) for their very helpful advice during the initial phase of the project.

Supporting information for this article is available on the WWW under http://dx.doi.org/10.1002/anie.201201866.

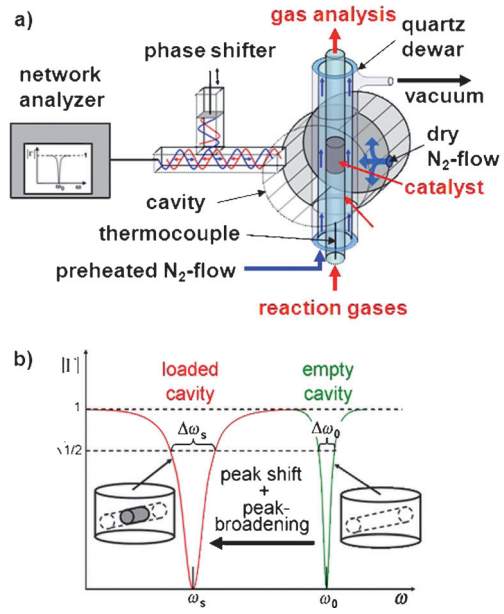


***Figure 1.*** a) Schematic of the MCPT/GC setup using the $TM_{110}$ mode at 9.2 GHz of a cylindrical cavity allowing the investigation of powder catalysts in a fix-bed flow-through quartz reactor under reaction conditions. Sample heating is enabled by an external gas heating element. b) Measurement principle of MCPT. Shown is the reflection factor versus frequency for critical coupling with and without sample. By measuring the frequency shift $(\omega_s-\omega_0)$ and the change of the line width with and without sample $(\Delta\omega_s-\Delta\omega_0)$ the complex permittivity and electrical conductivity can be calculated: $(\omega_s-\omega_0)/\omega_0=A(\varepsilon_1-1)V_s/V_c$; $(\Delta\omega_s-\Delta\omega_0)/\omega_0=B\varepsilon_2V_s/V_c$; $\sigma=\varepsilon_0\varepsilon_2\omega_s$. *A* and *B* are calibration constants, and $V_s$ and $V_c$ are the sample and the cavity volume.

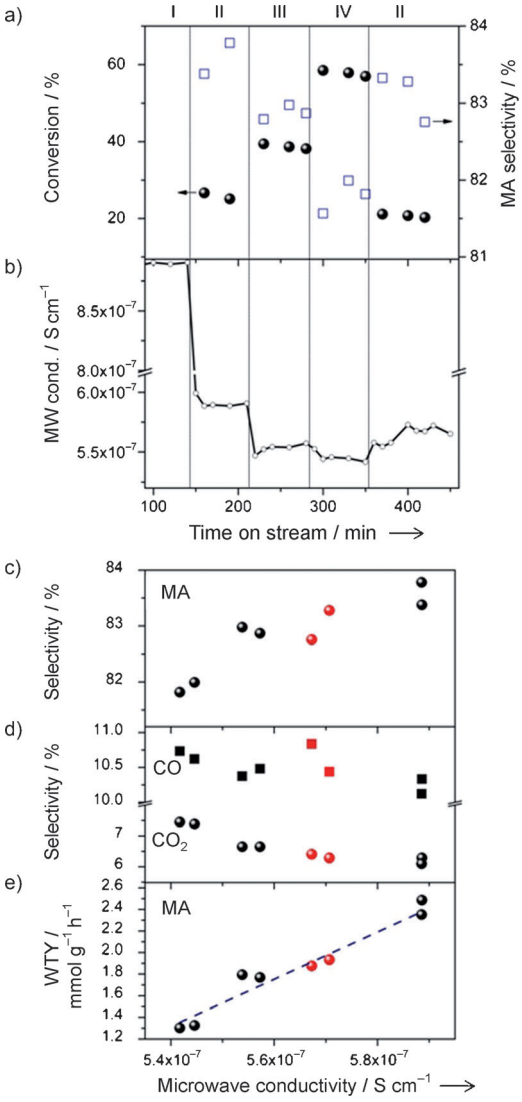


***Figure 2.*** Conversion of *n*-butane and MA selectivity (a) and microwave conductivity (b) in different gas atmospheres and at different GHSVs. Conditions: I: 100% $N_2$, GHSV: 14150 $h^{-1}$; II: 2% *n*-$C_4H_{10}$, 20% $O_2$ in $N_2$, GHSV: 14150 $h^{-1}$; III: 2% *n*-$C_4H_{10}$, 20% $O_2$ in $N_2$, GHSV: 7075 $h^{-1}$; IV: 2% *n*-$C_4H_{10}$, 20% $O_2$ in $N_2$, GHSV: 3540 $h^{-1}$. MA selectivity (c), CO and $CO_2$ selectivity (d), and weight time yield (WTY) of MA (e) relative to the determined microwave conductivity for conditions II–IV. The dashed line is a linear-regression fit. Red symbols are values for the relaxed catalyst after switching from condition IV to II. In (c)–(e) all the values are steady-state values (in each case the last two measurement points in (a)).

14150 $h^{-1}$) followed by an isothermal treatment in 100% $N_2$ (condition I; Figure 2a,b). After 100 min the measured conductivity leveled at $8.9\times10^{-7}$ S cm$^{-1}$. Subsequently, a lean reaction-gas mixture containing 2% *n*-butane in air at 14150 $h^{-1}$ was introduced (condition II). As a result, the conductivity declined sharply while a conversion between 25 and 27%, and a MA selectivity between 83.4 and 83.8% was determined (Figure 2a,b). Then, the GHSV was successively changed to 7075 $h^{-1}$ (condition III), 3540 $h^{-1}$ (IV), and back to 14150 $h^{-1}$ (II). As a consequence, with decreasing GHSV an increasing conversion and both a decreasing MA selectivity and conductivity were obtained. After switching the GHSV back to 14150 $h^{-1}$, neither the catalytic performance nor the conductivity fully recovered. Instead, a lower conversion, MA selectivity, and conductivity were determined.

Plotting the MA, CO, $CO_2$ selectivities and the MA production rate as weight-time-yield (WTY) versus conductivity suggests that a high conductivity favors a high MA selectivity and rate (Figure 2c–e), but a low total-oxidation product ($CO_x$) selectivity. Moreover, the rate of MA formation depends approximately linearly on the MW conductivity of the working catalyst (Figure 2e). Noteworthy, the final state of the relaxed catalyst after increasing the GHSV back to 14150 $h^{-1}$ fits nicely into this monotonic dependence, further supporting the intimate relationship between electronic and catalytic behavior.

If the often proposed first and rate-determining step of the reaction, that is, the oxy-dehydrogenation of butane to butyl and finally butene,[3,13,19,23] is considered, the dependence of the rate on the number of majority charge carriers (holes in p-semiconductors: $h^\bullet$) and hence conductivity, that is, $r\propto[h^\bullet]\propto\sigma$, can be explained through Equation (1) (in Kröger-Vink notation[11]).

$$C_4H_{10:(ads)} + O_O^x + h^\bullet \rightarrow C_4H_{9:(ads)}^{\cdot} + OH_O^\bullet \quad (1)$$

  

Long contact times increase the consumption of starting materials, indicated by a higher conversion. The thus lower starting-material concentration causes the rate of product formation to decrease. Hence, the direct change in conductivity (proportional to charge-carrier concentration) with contact time can be explained by the consumption of charge carriers during the reaction. Moreover, the negative correlation between conductivity and $CO_x$ selectivity can be explained by a lower availability of selective (lattice) oxygen at high contact times (i.e. at low conductivities), this then favors total oxidation by electrophilic oxygen species (e.g. $O_2^-$ and $O^-$) on the catalyst surface.[24]

In addition, in situ X-ray photoelectron spectroscopy (XPS) was performed to elucidate the catalyst surface and sub-surface electronic structure. In previous investigations, in situ XPS and in situ X-ray absorption of VPP indicated major differences between the electronic structure of the topmost surface and deeper layers.[25–27] It has been proposed that the gas-phase chemical potential sets the boundary conditions for the formation of a distinct surface phase. We measured in situ XPS of the VPP sample in a reaction cell allowing the monitoring of product gases with proton-transfer-reaction mass spectrometry (PTR-MS). First, a lean reaction gas mixture ("C4/O2": 0.5 sccm *n*-$C_4H_{10}$, 5.0 sccm $O_2$) was introduced. At 320 °C a strong initial rise of the MA PTR-MS signal at *m/e* 99, and a subsequent decrease to a constant lower level was observed (Figure 3a). While the initial MA peak can be explained by the desorption of residual MA from the catalyst, the subsequent constant MA rate can be attributed to a real continuous MA production. The consumption of *n*-butane was too low to be measured by the applied analytical equipment, that is, the conversion was below 1%. However, the experiment clearly showed that the catalyst was working under the applied conditions (total pressure in reaction cell: 0.5 mbar). At 400 °C, the increasing MA signal in the PTR-MS response indicates a much higher *n*-butane turnover (Figure 3a). Simultaneously, XP spectra were acquired. First, photoelectrons up to an information depth of 1.4 nm were detected (for details see Supporting Information). From the evaluation of the recorded V $2p_{3/2}$ spectra (Supporting information, Figure S3) average vanadium oxidation states were deduced (Figure 3b). After applying an oxidizing gas mixture ("O2/He": 5.0 sccm $O_2$, 0.5 sccm He) an increase of the V oxidation state from 4.25 to 4.31 was observed. Switching to the reducing mixture ("C4/He": 0.5 sccm *n*-$C_4H_{10}$, 5.0 sccm He) induced a decrease to 4.07. Additionally, average V oxidation states from an information depth between 1–4 nm representing sub-surface layers were determined (more details in the Supporting Information). Accordingly, sub-surface oxidation states of 4.09, 4.10, and 4.02 were observed in the mixtures "C4/O2", "O2/He", and "C4/He", respectively (Figure 3b). After switching back to the lean reaction mixture "C4/O2" the MA rate recovered and the average oxidation state of vanadium approached with 4.27 (surface) and 4.07 (sub-surface), respectively, the original values.

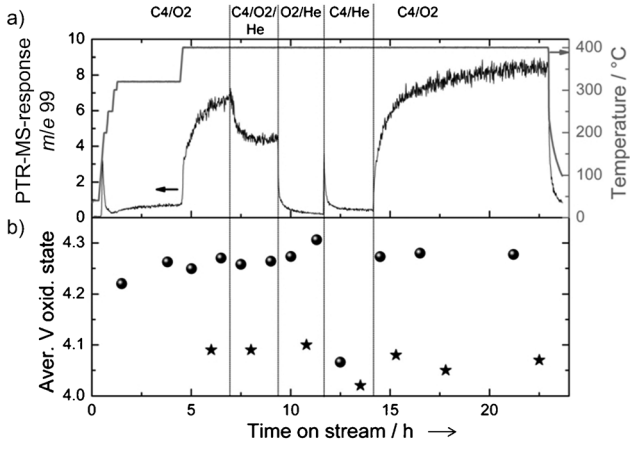


***Figure 3.*** a) PTR-MS signal of MA and applied temperature program in different gas mixtures at 0.5 mbar. b) Average V oxidation state in VPP obtained at different depths as determined by the evaluation of the V $2p_{3/2}$ core level. ● Surface region, measured within 1.4 nm information depth. ⋆ Sub-surface region, measured in approximately 1–4 nm depth (for details, see the Supporting Information). Gas mixtures: "C4/O2" 0.5 sccm *n*-$C_4H_{10}$, 5.0 sccm $O_2$; "C4/O2/He" 0.5 sccm *n*-$C_4H_{10}$, 2 sccm $O_2$, 3 sccm He; "O2/He" 5.0 sccm $O_2$, 0.5 sccm He; "C4/He" 0.5 sccm *n*-$C_4H_{10}$, 5.0 sccm He.

Three major findings can be deduced from the in situ XPS measurements: 1) The surface of the VPP catalyst is highly dynamic and the average vanadium oxidation state can fluctuate between 4.0 and 4.3. This result corresponds to the dynamic microwave conductivity response (Figure S2, in the Supporting Information). In a first approximation, the conductivity depends on the abundance of $V^{5+}$. This dependence could be explained by the rigid band model assuming $(VO)^{3+}$ as acceptor states[28] inducing electron holes in the VPP valence band upon thermal ionization [Eq. (2)]:

$$(V^{V}O)^{\bullet}_{VO} \rightleftharpoons (V^{IV}O)^{x}_{VO} + h^{\bullet} \quad (2)$$

2) The dynamic response of the V oxidation state is only observed in the surface region, whereas even at a depth of just 1–4 nm the V oxidation state is very close to the bulk value of 4.0. 3) The redox processes are completely reversible.

However, it is very questionable that the dynamic behavior and the high surface concentration of $V^{5+}$ can be accommodated by a perfect surface termination as part of the translational symmetric VPP lattice. Moreover, in the "C4/O2" lean reaction gas mixture at 400 °C a surface V:P:O ratio of 1:1.5:6 was determined by XPS. These values deviate significantly from the theoretical 1:1:4.5 ratio of the Daltonid formula $(VO)_2P_2O_7$. In particular the high excess of surface oxygen atoms points to a surface phase-segregated state consisting of a metastable two-dimensional binary vanadium oxide (and phosphoric acid).[25]

Although the site-isolation concept, demanding a (by the reaction stoichiometry) restricted number of well separated active oxygen surface species,[12–14] is in agreement with these results, it seems to conflict with the observed dependence of the rate on the bulk conductivity, especially if a rigid *band* model with delocalized bands is used to describe the conductivity. Hence the dynamic conductivity should be better explained by the involvement of (local) surface states. From the in situ XPS results, such surface states can

  

be identified as part of the $V_xO_y$ surface reconstruction resulting from metastable termination of VPP under reaction conditions. The lowest unoccupied and highest occupied molecular orbitals of surface states are usually situated within the band gap of the bulk semiconductor.[15,28] As a consequence, a charge transfer between bulk and surface state will occur inducing band bending and the formation of a space charge region (Figure 4). The band bending will manifest

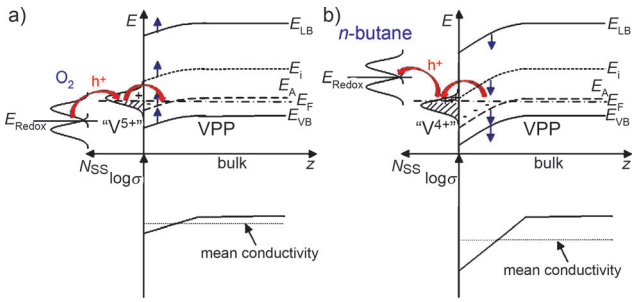


***Figure 4.*** Band diagram of p-type semiconductor with upward band bending upon adsorption of the acceptor molecule $O_2$ at surface states (SS) (a) and downward bending upon adsorption of the donor *n*-butane (b). In VPP, the emptied surface state would correspond to $V^{5+}$, the occupied surface state would correspond to $V^{4+}$. $E_F$: Fermi energy, $E_i$: intrinsic energy, $E_{CB}$: conduction band edge, $E_{VB}$: valence band edge, $E_A$: energy of bulk acceptors. The arrows indicate the transfer of electron holes (red) and the change of the band bending (blue) arising from adsorption of molecules with suitable frontier orbitals and redox energies $E_{Redox}$ at surface states. Additionally, the corresponding local and mean conductivity (as measured by integral methods such as MCPT) of the semiconductor are shown schematically.

itself in a conductivity response arising from the change of the charge-carrier concentration in the space charge region. If an (electron) acceptor molecule with matching energy and symmetry of its frontier orbitals, for example, $O_2$, adsorbs at a surface state of the p-type semiconductor VPP, the number of electron holes in the space charge region (upward bending, decrease of the hole depletion layer or formation of an accumulation layer) and thus the conductivity will be increased (Figure 4a). In contrast, adsorbing donors, such as $H_2$ or *n*-butane, will induce a downward bending and consequently reduce the number of holes and the conductivity (Figure 4b). By the identification of the surface states as catalytically active sites, the unambiguous bulk conductivity response can be explained, that is, the catalyst acts like a solid-state gas sensor (chemiresistor).[29] VPP with its isolated polymeric $[V_2O_4]$ chains perpendicular to the {100} plane provides an optimal structure to facilitate the bulk–surface charge transfer. However, the observed conductivity response indicates that the charge transfer to the surface is limited by the reaction-induced formation of a hole-depletion layer (and thus increasing electrostatic repulsion within this layer). The phenomenon of a space charge restricted charge transfer would be in conceptual agreement with the site-isolation principle.

In summary, the first-time application of the noncontact microwave cavity perturbation technique for studying the dynamic electrical conductivity of VPP catalysts in the oxidation of *n*-butane revealed 1) a charge transfer between bulk and surface during the oxidation reaction arising from the direct response of the measured conductivity to the reaction-gas contact time, 2) a positive correlation between conductivity and MA production rate, and 3) a reversed response of the $CO_x$ selectivities upon conductivity changes. Furthermore, in situ XPS studies showed that the reversible oxidation-state change of the $V^{4+}/V^{5+}$ redox couple is restricted to the topmost surface layers. The hence unexpected sensitivity of the measured bulk conductivity on changes at the catalyst surface can be explained by a space charge limited bulk–surface charge transfer. This concept implies the presence of local ($V^{4+}/V^{5+}$) surface states as the active sites for the oxidation reaction, resolving the apparent conflict between the site-isolation principle and the participation of bulk charge carriers.

Received: March 8, 2012
Published online: May 8, 2012

**Keywords:** electrical conductivity · heterogeneous catalysis · in situ spectroscopy · oxidation

[1] C. H. Bartholomew, R. J. Farrauto, *Fundamentals of Industrial Catalytic Processes*, 2nd ed., Wiley-Interscience, Hoboken, NJ, **2006**.
[2] M. A. Pepera, J. L. Callahan, M. J. Desmond, E. C. Milberger, P. R. Blum, N. J. Bremer, *J. Am. Chem. Soc.* **1985**, *107*, 4883–4892.
[3] G. Centi, F. Trifiro, J. R. Ebner, V. M. Franchetti, *Chem. Rev.* **1988**, *88*, 55–80.
[4] G. Centi, *Catal. Today* **1993**, *16*, 5–26.
[5] J. C. Volta, *C. R. Acad. Sci. Ser. IIc* **2000**, *3*, 717–723.
[6] N. Ballarini, F. Cavani, C. Cortelli, S. Ligi, F. Pierelli, F. Trifiro, C. Fumagalli, G. Mazzoni, T. Monti, *Top. Catal.* **2006**, *38*, 147–156.
[7] M. Abon, K. E. Bere, P. Delichere, *Catal. Today* **1997**, *33*, 15–23.
[8] U. Rodemerck, B. Kubias, H. W. Zanthoff, M. Baerns, *Appl. Catal. A* **1997**, *153*, 203–216.
[9] D. X. Wang, H. H. Kung, M. A. Barteau, *Appl. Catal. A* **2000**, *201*, 203–213.
[10] M. J. Lorences, G. S. Patience, F. V. Diez, J. Coca, *Appl. Catal. A* **2004**, *263*, 193–202.
[11] P. J. Gellings, H. J. M. Bouwmeester, *Catal. Today* **2000**, *58*, 1–53.
[12] R. K. Grasselli, *Top. Catal.* **2001**, *15*, 93–101.
[13] J. C. Volta, *Top. Catal.* **2001**, *15*, 121–129.
[14] R. K. Grasselli, *Top. Catal.* **2002**, *21*, 79–88.
[15] J. Haber, M. Witko, *J. Catal.* **2003**, *216*, 416–424.
[16] F. Rouvet, J. M. Herrmann, J. C. Volta, *J. Chem. Soc. Faraday Trans.* **1994**, *90*, 1441–1448.
[17] J. M. Herrmann, P. Vernoux, K. E. Bere, M. Abon, *J. Catal.* **1997**, *167*, 106–117.
[18] M. Abon, J. M. Herrmann, J. C. Volta, *Catal. Today* **2001**, *71*, 121–128.
[19] J. M. Herrmann, *Catal. Today* **2006**, *112*, 73–77.
[20] L.-F. Chen, C. K. Ong, C. P. Neo, V. V. Varadan, V. K. Varadan, *Microwave Electronics: Measurement and Materials Characterization*, Wiley, Hoboken, **2004**.
[21] O. Klein, S. Donovan, M. Dressel, G. Grüner, *Int. J. Infrared Millimeter Waves* **1993**, *14*, 2423–2457.

  

[22] M. Eichelbaum, R. Stößer, A. Karpov, C.-K. Dobner, F. Rosowski, A. Trunschke, R. Schlögl, *Phys. Chem. Chem. Phys.* **2012**, *14*, 1302 – 1312.
[23] J. M. M. Millet, *Top. Catal.* **2006**, *38*, 83 – 92.
[24] S. Pradhan, J. K. Bartley, D. Bethell, A. F. Carley, M. Conte, S. Golunski, M. P. House, R. L. Jenkins, R. Lloyd, G. J. Hutchings, *Nat. Chem.* **2012**, *4*, 134 – 139.
[25] H. Bluhm, M. Hävecker, E. Kleimenov, A. Knop-Gericke, A. Liskowski, R. Schlögl, D. S. Su, *Top. Catal.* **2003**, *23*, 99 – 107.
[26] M. Hävecker, R. W. Mayer, A. Knop-Gericke, H. Bluhm, E. Kleimenov, A. Liskowski, D. Su, R. Follath, F. G. Requejo, D. F. Ogletree, M. Salmeron, J. A. Lopez-Sanchez, J. K. Bartley, G. J. Hutchings, R. Schlögl, *J. Phys. Chem. B* **2003**, *107*, 4587 – 4596.
[27] E. Kleimenov, H. Bluhm, M. Hävecker, A. Knop-Gericke, A. Pestryakov, D. Teschner, J. A. Lopez-Sanchez, J. K. Bartley, G. J. Hutchings, R. Schlögl, *Surf. Sci.* **2005**, *575*, 181 – 188.
[28] S. R. Morrison, *The Chemical Physics of Surfaces*, Springer, New York, **1990**.
[29] M. E. Franke, T. J. Koplin, U. Simon, *Small* **2006**, *2*, 36 – 50.

  